OUTCOME OF THE AVAILABLE 2D MCCI EXPERIMENTAL DATABASE FOR THE REACTOR CASE IN DRY CONDITIONS

Authors: M. Cranga, B. Michel, C. Mun, M. Barrachin
Institut de Radioprotection et de Sûreté Nucléaire, IRSN, DPAM, SEMIC
13115 St Paul Lez Durance, France

Tél. : +(33) 4 42 19 94 82, Fax : +(33) 4 42 19 91 67, E-mail : michel.cranga@irsn.fr

This work updates and completes the study presented at the last MCCI seminar in 2007 [1]. The purpose of the present work is to evaluate the impact of knowledge gained from MCCI-OECD and VULCANO experiments with real material performed during the last seven years and from the analysis of oxide/metal simulant experiments on reactor basemat melt-through delay in dry conditions. Some assumptions and models have been strengthened or developed or updated from the available experimental database and some theoretical works. They are capitalized in the ASTEC/MEDICIS code [2] developed by IRSN in collaboration with the German GRS organisation that has been used for the reactor calculations on a generic PWR900 reactor case using simplified but conservative boundary conditions presented in this article.

1 Outcome of past MCCI programs

Main findings obtained from the analysis and interpretation of MCCI experiments with real material and simulants are discussed briefly hereafter.

1.1 MCCI experiments in a homogeneous pool

The ratio of lateral over axial ablation observed in MCCI-OECD [3,4] and VULCANO [5,6] 2D MCCI tests strongly depends on the concrete type. A limestone sand concrete (LCS) promotes a rather homogeneous ablation whereas a siliceous concrete or any concrete releasing intact aggregates at ablation threshold promotes a lateral ablation.

The former analysis of 2D MCCI tests [7] leads to explain the dissymmetry of 2D ablation by the build-up of a solid accumulation at the cavity bottom generating an increased thermal resistance at this location in case of siliceous concrete. The heat transfer towards the pool/concrete interface was described in ASTEC/MEDICIS using the concept of a solidification temperature $T_{solidif}$ determining the interface temperature between the convective bulk pool zone and a conductive zone (or mushy crust) as indicated in next figure 1.

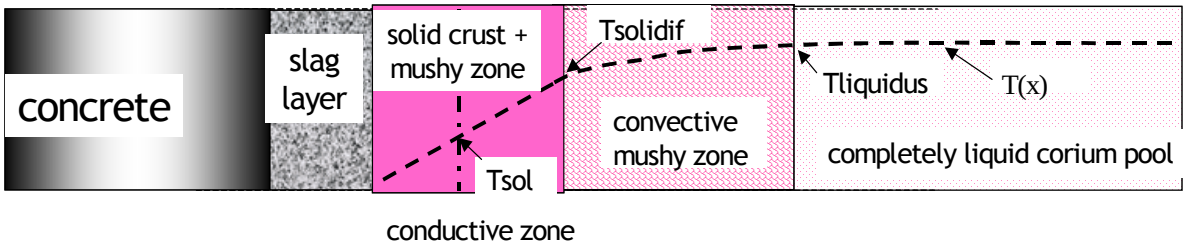

Fig. 1: Pool/concrete interface structure in case of model 1

The increased thermal resistance at the bottom interface in case of siliceous concrete was described by increasing the resistance of the slag layer (or equivalently decreasing the hslag heat transfer coefficient) leading to the suppression of the intermediate conductive zone. In case of a LCS concrete, the same interface structure was kept for all pool/concrete interfaces assuming a low thermal resistance of the slag layer (or equivalently a high hslag heat transfer coefficient). This approach permitted to reproduce roughly the evolution of pool temperature and 2D concrete ablation for both concrete types. The draw-back of this approach is to assume an interface structure related at least indirectly to corium solidification along the lateral pool/concrete interface: indeed the long term stability of a vertical conductive mushy zone or crust is unlikely in particular in presence of gas bubbling and of release of intact aggregates during ablation.

Generally speaking, the evaluation of the inner temperature of a boundary layer (called solidification temperature in the previous approach) from thermochemistry data obtained for the average pool composition is not consistent with the complex structure of phases and the absence of any uniform zone near the pool/concrete interface, as deduced for example from post-test examinations (PTE) for VBU5 and VBU6 VULCANO tests for both concrete types.

Besides, up to now no direct information on the crust existence and stability can be derived from real material experiments.

Therefore a new very simple modelling is proposed to account for the 2D ablation anisotropy: this consists of assuming that no stable crust even in mushy state can build-up at a given solidification temperature along the pool/concrete interface whatever the concrete type. The heat transfer from the bulk pool to the concrete interface is determined only by convection in the bulk pool and heat transfer at the interface. The interface thermal resistance depending on the interface orientation is imposed using the hslag heat transfer coefficient, as indicated in figure 2. This permits to model a simple slag layer made of concrete oxides or a solid accumulation or an inert crust without any link with a solidification temperature.

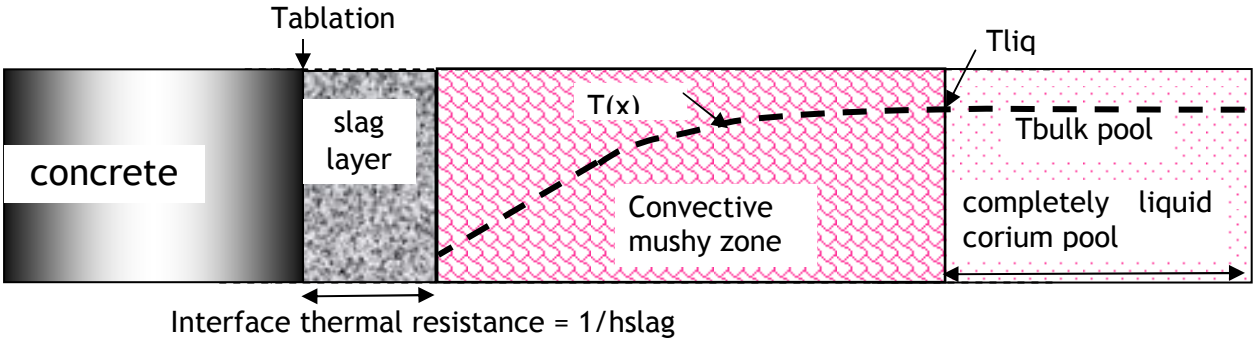

Fig. 2: Pool/concrete interface structure in case of model 2

More recent VULCANO experiments confirmed the prevailing influence of the aggregate behaviour at the ablation temperature [8]. This influence might be easily explained qualitatively in the frame of the new modelling: still intact aggregates are easily released at the lateral interface keeping a low thermal resistance whereas the released aggregates at the bottom interface might pile up below the solid accumulation or crust built-up early in the experiment increasing thus the thermal resistance.

The concept of solidification temperature is kept in the new modelling approach only to evaluate the interface temperature between the bulk pool and the upper crust at the upper pool interface. In the former recalculations of 2D MCCI experiments the solidification temperature was evaluated from liquidus and solidus temperature using the formula

$$T_{solidif} = \gamma.T_{solidus} + (1-\gamma).T_{liquidus},$$

where the γ interpolation parameter stands between 0.2 and 0.4. However the draw-back of this criterion is to have a lack of physical basis and to overestimate very often the upper crust thickness. Therefore a new more physical criterion is evaluating the solidification temperature from a volumetric liquid fraction obtained by an interface with the NUCLEA thermochemistry database [17] and corresponding to a corium mobility threshold of 0.5 [9]; this criterion leads to a thinner and more realistic upper crust thickness.

This new approach was applied on some 2D MCCI experiments and permitted in case of siliceous concrete to reproduce main experimental data fitting the profile of the hslag heat transfer coefficient in the slag layer along the concrete interface with a hslag value equal to 80 $W/m^2/K$ at the cavity bottom interface to model a stable solid accumulation and to 300 $W/m^2/K$ at the cavity lateral interface to model a boundary layer without crust [9]. In case of the LCS concrete, the new approach using a uniform hslag heat transfer coefficient in the slag layer along the concrete interface with a hslag value around 300 $W/m^2/K$ permitted to reproduce correctly main data in case of CCI2. In all recalculations of experiments, the convective heat transfer coefficient was considered to be independent of the orientation of the interface. The same type of approach is applied below to the reactor-case.

1.2 Experimental data on the oxide/metal pool during MCCI

The recent VULCANO VBS-U experiments performed with an oxide/metal pool [10, 11] lead to following results: a large fraction of the iron was oxidized during the test even in case of the VBS-U3 test with siliceous concrete; post-test examinations showed some metal rich accumulations along the lateral interface, in case of the VBS-U3 test in particular. However they did not permit up to now to conclude clearly on the occurrence of oxide/metal stratification.

As far as simulant experiments are concerned, recent analyses of ABI experiments [12] confirmed that the convective heat transfer at the oxide/metal interface in a stratified pool is high compared to the convective heat transfer coefficient towards the lateral oxide/concrete interface. The review of available data on stratification criteria [12] showed also that the criterion on superficial gas velocity

corresponding to the full mixing of layers derived from BALISE experiments [14] is overestimated especially for a low ratio of metal to oxide masses. The use of a lower superficial gas velocity threshold corresponding to the onset entrainment of heavier liquid should be more realistic and is used below.

2 Reactor applications

A set of sensitivity calculations using the ASTEC/MEDICIS code have been performed on a typical PWR900 MWe reactor. Results on the basemat ablation kinetics are presented here taking into account the two different heat transfer models at the pool/concrete interface (models 1 and 2 described above) and at the upper pool interface, with and without pool configuration evolution, and at low and high pressure in the cavity. These calculation results taking into account the outcome of the whole set of available MCCI experiments including simulant ones are likely to be more realistic compared to those presented at the previous MCCI seminar in 2007 for dry conditions [1].

2.1 Choice of boundary conditions, assumptions and models

Features of a typical PWR900 MWe reactor are chosen. Calculation conditions are selected to get conservative results. The impact of an earlier lateral melt-through time on the axial ablation progression is ignored and no limitation of lateral erosion is considered. Data for the reactor geometry, material compositions, initial and boundary conditions are displayed on table 1.

initial oxidic corium inventory (t)	UO2 mass: 82, ZrO2 mass: 19.5
initial metallic corium inventory (t)	Zr: 4.8, Fe: 35, Ni:4, Cr:6
reactor pit radius	3m
basemat axial thickness	3m to 4m
concrete characteristics	reinforced siliceous or limestone-sand concrete (LCS) with 6.5% Fe due to iron bars
vessel failure time	1h after scram
time after scram, decay power (W/kg U)	1h: 283, 3h: 227, 7h: 190, 15h: 157, 20h: 145, 50h: 108, 9d: 63
initial corium temperature	2673K (the oxide phase is solid)
upper pit wall temperature	1700K or 1500K (in variants)
Pressure in reactor pit	low pressure in basic cases: constant equal to 1.5 bar higher pressure in variants: evolving versus time : t=0h: 1.5bar, t=10h: P=2bar, t=20h: P=3bar,t= 5,7days: 5bar

Table 1: reactor features, initial and boundary conditions for MCCI calculations.

The total degraded core inventory is assumed to be present in the reactor pit at the reactor vessel failure. The upper reactor pit structure temperature is set to a constant value (1700K) near the steel melting point; this assumption is then conservative since it leads to underestimate the power radiated by the corium pool towards the reactor pit walls. In case of a lower solidification temperature used in variant calculations (see next table 2), the pool temperature might decrease below the temperature of the upper structures ; in order to avoid such an unrealistic boundary condition, the temperature of the upper structures is set to the lower level of 1500K, which is near the concrete ablation temperature and quite realistic.

The pool/concrete interface model determines the thermal resistance of the pool/concrete interface and thus the local convective heat flux. Taking advantage of the ASTEC/MEDICIS code flexibility, two different interface models are used in present calculations. The first interface model of the pool/concrete interface structure used in previous analyses [7] is schematized on fig.1. Heat is transported by gas bubbling across this pool mushy zone and then, as the solid fraction is high enough, by conduction to the concrete ablation interface. The temperature of the boundary between pool conductive and convective zones is the solidification temperature. The slag layer heat transfer coefficient value is kept here constant and equal to a high value ($1000 W/m^2/K$) to simulate a low interface thermal resistance and maintain the stability of the conductive zone. In the second interface model of the interface structure, no conductive zone is present and the slag layer heat transfer value determines the overall thermal resistance across the interface. This latter model is used to describe on a simplified way the built-up at the bottom pool interface of a solid accumulation increasing the thermal resistance while keeping a lower thermal resistance along the lateral interface.

Model options and values of key model parameters used in MEDICIS are summed-up in table 2.

pool configuration	homogeneous, stratified, with configuration evolution
pool/concrete interface structure	1)first model for both concrete types: build-up of conductive zone at solidification temperature + uniform slag layer heat transfer coefficient equal to 1000 $W/m^2/K$ 2)second model: no conductive zone or crust along the concrete interface ; hslag slag layer heat transfer coefficient: in case of siliceous concrete, hslag profile versus angle with value at the bottom interface of the oxidic layer (and also of the metal layer in case of variant) equal to 80 $W/m^2/K$ and maximum lateral value equal to 300 $W/m^2/K$; in case of LCS concrete, hslag is uniform equal to 300 $W/m^2/K$
heat convective coefficient at oxide and metal concrete interface	Bali's correlation [15] for convective heat transfer to all concrete interfaces
heat transfer at oxide/metal interface	Convective heat transfer coefficient determined by Greene's correlation [13] on each interface side + possible oxidic corium solidification on the oxide layer side at the solidification temperature
solidification temperature	either $T_{solidif} = \gamma.T_{solidus} + (1-\gamma).T_{liquidus}$ with γ =0.2 or $T_{solidif} = Fvol,liq^{-1}(0.5)$ (in variant of the second model)
configuration evolution	strat. => homog. config. switch : Jg > (ρ_{bot} - ρ_{top})/ ρ_{bot} m/s or metal layer thickness < 3 10^{-2}m homog. => strat. config. switch : Jg < 0.027 (ρ_{bot} - ρ_{top})/ ρ_{bot} m/s and metal layer thickness > 3 10^{-2}m

Table 2: assumptions and choices of models

The Jg threshold value for the switch from an homogeneous configuration to a stratified one has a large impact; to get a realistic evaluation of this threshold, it is assumed to correspond to the onset of entrainment from the heavier phase into the lighter one derived from BALISE data [15] which is twice lower than the original BALISE criterion [12], which was used in the previous parametric study [1]. The threshold value of superficial gas velocity (Jg) for the switch from stratified to homogeneous configuration is chosen high enough to hinder any premature switch back after the pool stratification, which is conservative.

The minimum metal thickness permitting stratification was chosen equal to 3cm, because this is higher than the maximum gas bubble size in the corium pool and low enough to trigger a complete mixing of layers: indeed the analysis of available stratification criteria [12] shows a strong reduction of the superficial gas velocity threshold with the decrease of metal to oxide volume ratio ; in particular Epstein's criterion [16] for full mixing leads to a very low superficial gas velocity threshold below a few mm/s for a metal to oxide volume ratio below 1/50, which is the case for a metal layer thickness below 3cm in the long term MCCI phase.

2.2 Results for siliceous concrete

The study is focussed on the influence of the choice of the interface structure model (1 or 2) taking into account or not the pool configuration evolution.

2.2.1 Results at low pressure

Results obtained for a low pressure are presented below.

First let us have a look at the case assuming a homogeneous pool configuration. The modelling of the interface structure without stable crust and an increased heat transfer at the bottom interface (second model) leads to huge lateral ablation (fig.2) compared to the calculation with first model assuming a uniform interface structure and to a very late melt-through of several tens of days.

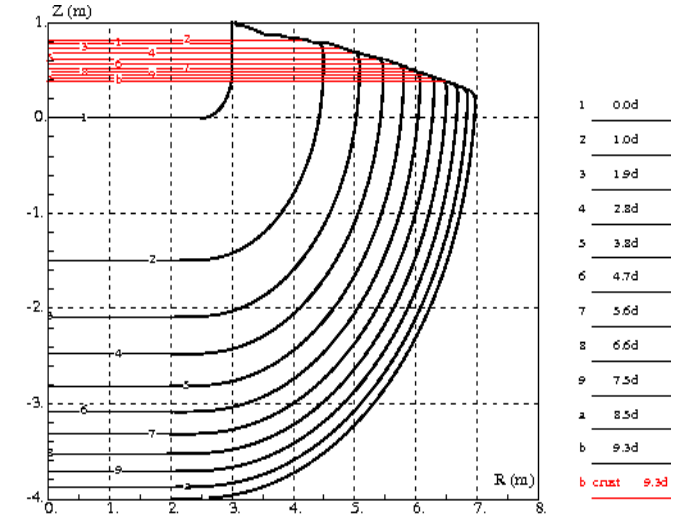

Homogeneous config., siliceous concrete basemat

uniform thermal resistance with crust at interface

Fig.1: cavity evolution in case of siliceous concrete: case with homogeneous pool configuration and interface structure model 1 tmth= 9.3 days

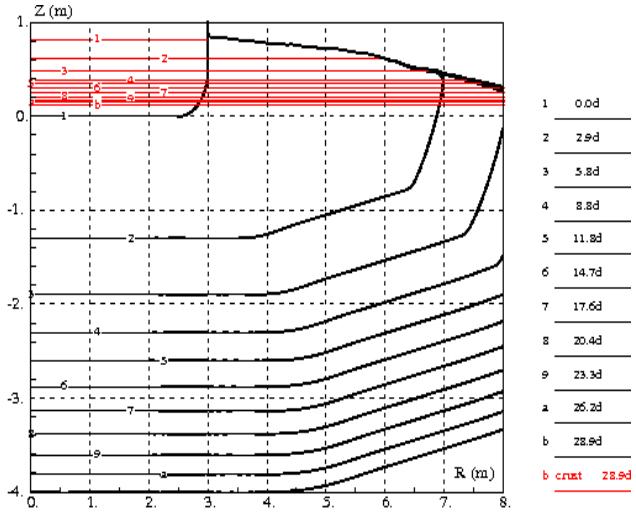

Homogeneous config., siliceous concrete basemat

higher thermal resistance at cavity bottom

Fig.2: cavity evolution in case of siliceous concrete case with homogeneous configuration and interface structure model 2 tmth= 28.9 days

Now let us consider the cases taking into account the pool configuration evolution. If using the interface model 1, the stratification with metal below leads to a rather early melt-through due to the isotropic ablation during the homogeneous pool configuration phase (fig.3). However the use of the interface model 2 increases the lateral ablation mainly once the homogeneous pool configuration is definitely recovered after suppression of stratification and delays the melt-through considerably (fig.4).

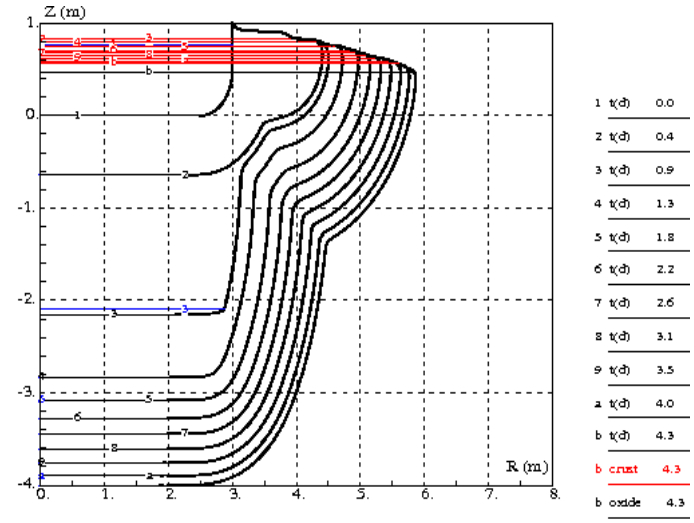

Reference case: hslag = 1000 W/m2/K, stable crust in oxide

Stratification criteria: bHS = 0.027, metthick > 3cm

Fig.3: cavity evolution in case of siliceous concrete: case with pool configuration evolution and interface structure model 1 tmth= 4.3days

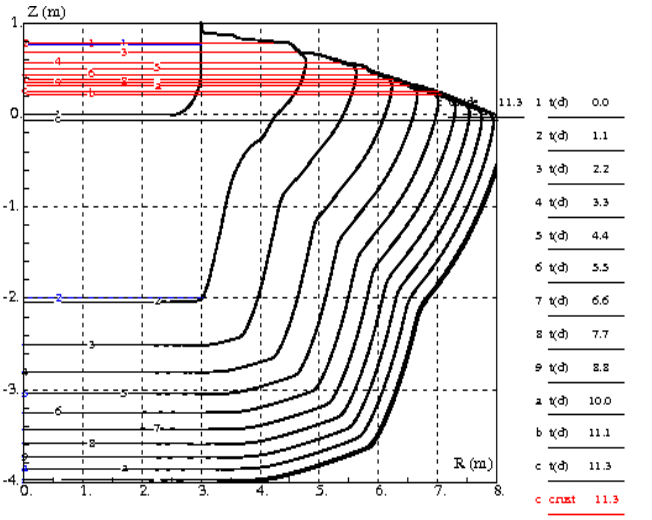

Hslag lateral 300, hslag bottom 80 W/m2/K Tsolidif(gam=0.2)

Stratification criteria: bHS = 0.027, metthick > 3cm

Fig.4: cavity evolution in case of siliceous concrete case with pool configuration evolution and interface structure model 2 tmth= 11.3 days

Finally let us investigate the influence of two model variants which may be derived from the analysis of available 2D MCCI experiments. These model variants are impacting respectively on the heat flux distribution along the pool/concrete interface and on the corium pool energy balance.

The first one assumes that the thermal resistance of the bottom interface possibly due to a solid refractory oxide accumulation is present not only at the oxide/concrete interface but also at the metal/concrete interface in the stratified pool phase with metal below; this variant might be more

realistic since the solid refractory oxide accumulation at the bottom interface should persist whatever the nature of melt above.

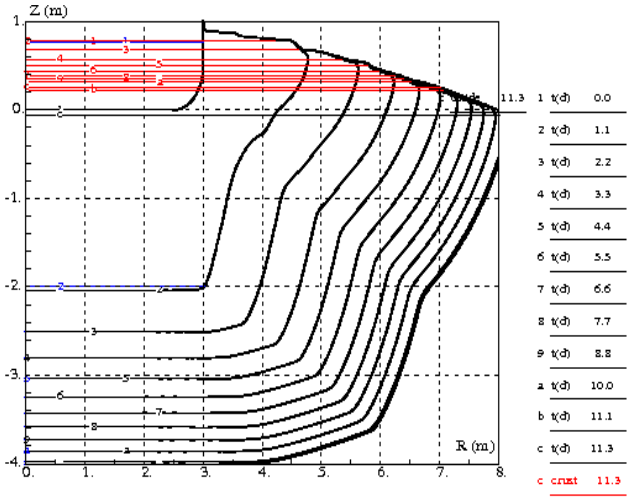

Hslag lateral 300, hslag bottom 80 W/m2/K Tsolidif(gam=0.2)
Stratification criteria: bHS = 0.027, metthick > 3cm

Fig.5: cavity evolution in case of siliceous concrete case with pool configuration evolution and interface structure model 2 tmth= 11.3 days

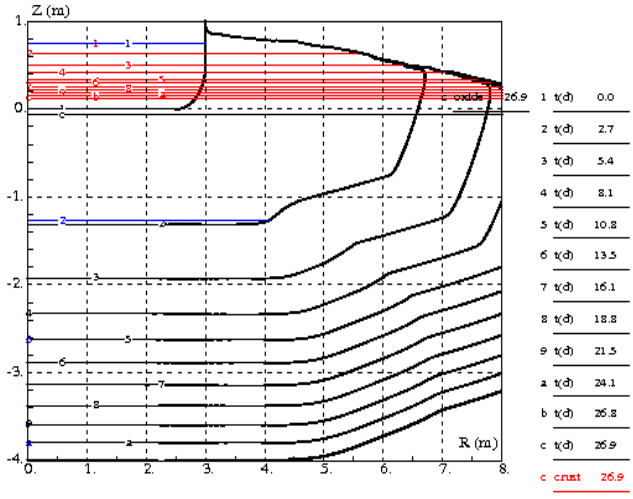

Hslag lateral 300, hslag bottom 80 W/m2/K in oxide and metal
Stratification criteria: bHS = 0.027, metthick > 3cm

Fig.6: cavity evolution in case of siliceous concrete with pool configuration evolution and interface structure model 2 variant: thermal resistance fct of angle both at oxide and metal/concrete interfaces tmth= 26.9 days

Comparison of fig. 6 with fig. 5 (identical to fig.4 and added here for comparison) shows a very clear change in the cavity evolution. Indeed the assumption of the presence of a solid accumulation both at the oxide and metal/concrete bottom interface increasing its thermal resistance reduces considerably the axial heat flux and axial ablation kinetics during the stratified pool phase with metal below. This causes a lateral heat redistribution enhancing the lateral ablation kinetics and leading a remarkably pronounced lateral ablation and a very late melt-through time near that obtained in the case with homogeneous pool ignoring the metal impact on pool stratification (see fig.2).

The second model variant concerns the evaluation of the solidification temperature used for determining the pool/upper crust interface temperature, which will impact on the upwards radiated power.

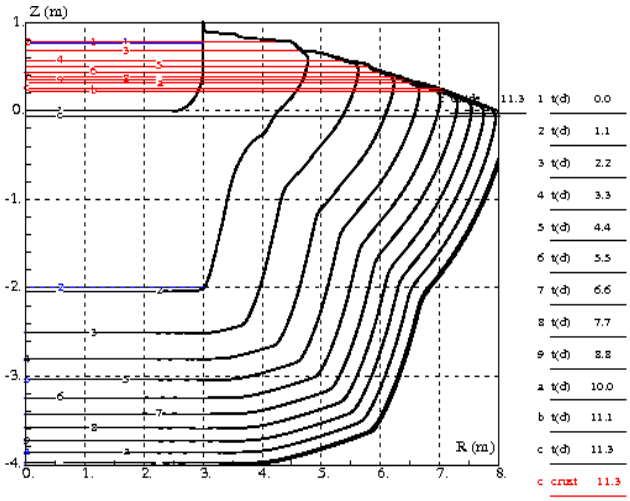

Hslag lateral 300, hslag bottom 80 W/m2/K Tsolidif(gam=0.2)
Stratification criteria: bHS = 0.027, metthick > 3cm

Fig.7: cavity evolution in case of siliceous concrete case with pool configuration evolution with interface structure model 2 tmth= 11.3 days

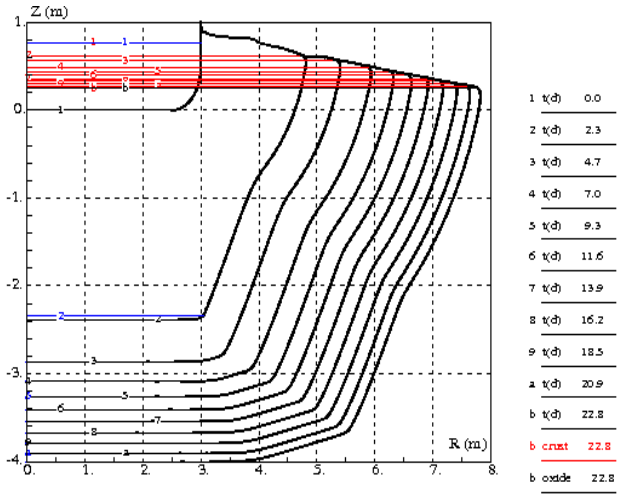

Hslag lateral 300, hslag bottom 80 W/m2/K, Tsolidif(Fvol=0.5)
Stratification criteria: bHS = 0.027, metthick > 3cm

Fig.8: cavity evolution in case of siliceous concrete case with pool configuration evolution, with interface structure model 2 variant: lower solidification temperature tmth= 22.8 days

Comparison of figure 8 with figure 7 (identical to fig.5 and added here for comparison) permits to point out the large impact of the reduction of the solidification temperature combined with the lower temperature of upper structures (1500K instead of 1700K). The reason is the absence of crust or conductive zone along the pool interface involving the solidification temperature in the evaluation of the pool/concrete heat flux: reducing the solidification temperature decreases only the upwards thermal resistance but does not change the thermal resistance of concrete interfaces which are imposed. This increases the fraction of power transferred upwards. Moreover due to the prevailing lateral ablation, the area of the pool upper interface becomes very large in the long term still enhancing the upwards radiated power.

2.2.2 Results at high pressure

Results obtained at higher pressure assuming a pool configuration evolution are displayed in next figures.

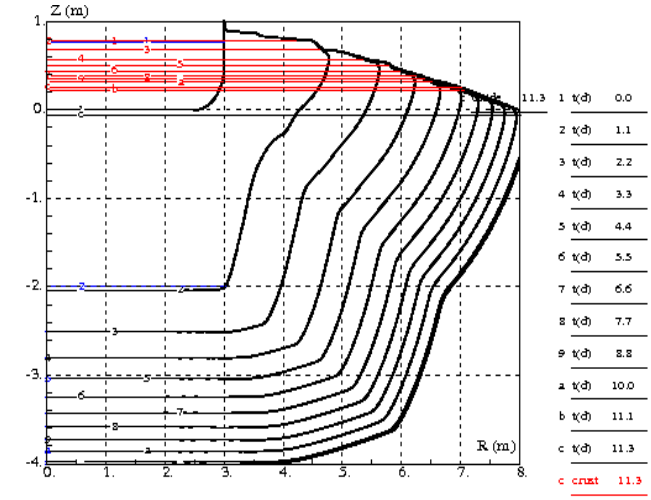

Fig.9: cavity evolution in case of siliceous concrete case with pool configuration evolution with interface structure model 2 tmth= 11.3 days

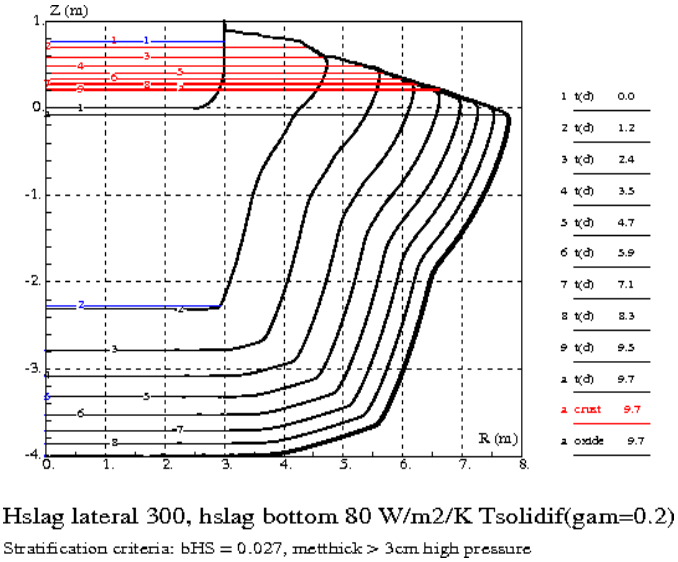

Fig.10: cavity evolution in case of siliceous concrete case with pool configuration evolution, with interface structure model 2 and high pressure tmth= 9.65 days

Results obtained at a higher pressure (see fig.10) show a slightly earlier melt-through compared to the similar case at lower pressure with interface structure model 2 (see fig.9 identical to fig.5 and added here for an easier comparison). The higher pressure decreasing the superficial gas velocity leads to a longer pool stratification phase but the impact remains moderate.

2.3 Results for a limestone-sand concrete

Some reactor applications in case of LCS concrete are presented for comparison with those concerning a siliceous concrete. According to the present state of knowledge, the ablation in the oxidic pool should be isotropic and at the opposite of siliceous concrete a uniform interface structure is very likely. The study considers here a uniform interface structure with pool configurations taking into account or not the pool configuration evolution. The first model with the formation of a conductive zone (or crust) at the solidification temperature along the concrete interface and the second model imposing a uniform thermal resistance without conductive zone along the pool/concrete interface and using for the build-up of the upper crust a solidification temperature determined a volumetric liquid fraction are successively considered.

Results obtained for a low pressure are presented below.

In case of homogeneous pool configuration with the first interface model (fig.11), the ablation is isotropic leading to an axial melt-through time close to that obtained with the same options in case of siliceous concrete (see fig.1). The impact of the second interface model leading also to an uniform heat flux profile along the concrete interface is low; however the choice of a lower solidification temperature and a lower upper wall temperature increases significantly the upwards radiated power thus delaying the melt-through (see fig.12).

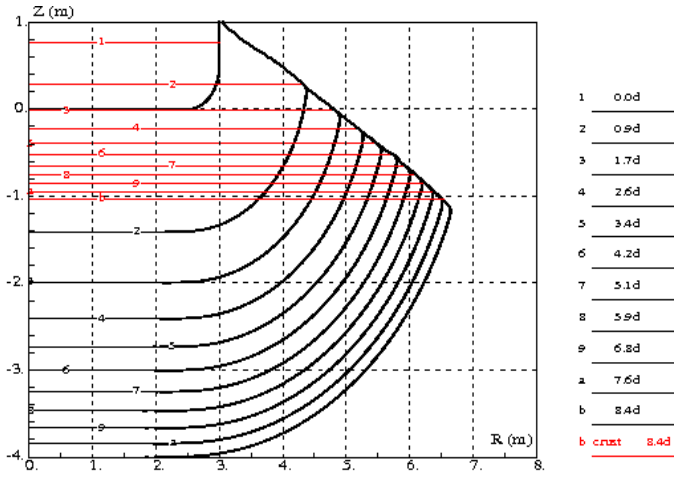

Homogeneous config., siliceous concrete basemat
uniform thermal resistance with crust at interface, Tsolidif(gam=0.2)

Fig.11: cavity evolution in case of LCS concrete: homogeneous pool, with interface structure model 1 tmth= 8.45 days

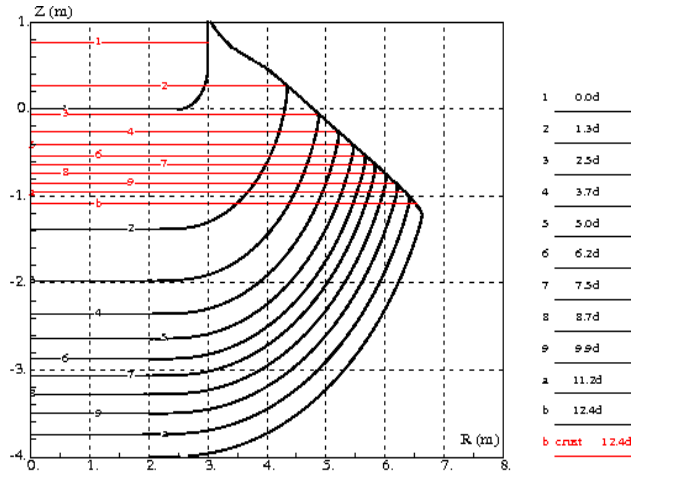

Homogeneous config., siliceous concrete basemat
hslaglat=300 W/m2/LK in oxide, Tsolidif(Flivol=0.5)

Fig.12: cavity evolution in case of LCS concrete: homogeneous pool with interface structure model 2 and lower solidification temperature tmth= 12.35 days

In case of pool configuration evolution (fig.13), the initial stratified pool configuration with metal above promotes a larger lateral ablation in a short first phase due the focussing of decay power along the lateral metal layer interface. Later due to the higher gas bubbling generated by ablation of LCS concrete, the superficial gas velocity is high enough to prevent any stratification with metal below. The consequence is a later axial melt-through than with homogeneous pool configuration (fig.9).

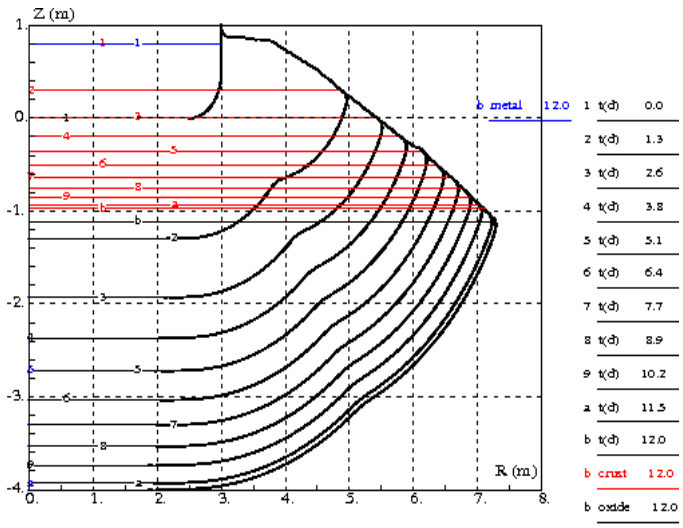

Reference case: with crust,Tsolidif(gam=0.2)
Stratification criteria: bHS=0.027, metthick > 3cm

Fig.13: cavity evolution in case of LCS concrete: pool configuration evolution with interface structure model 1 tmth= 11.96 days

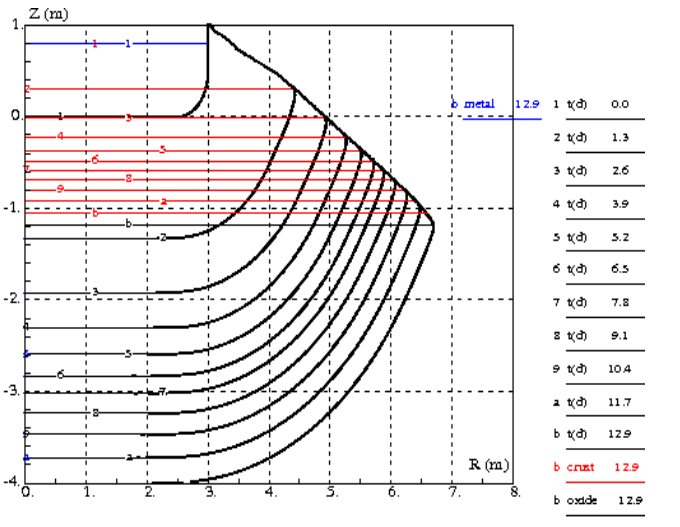

Hslag = 300 W/m2/K, Tsolidif(Fvol=0.5)
Stratification criteria: bHS=0.027, metthick > 3cm

Fig.14: cavity evolution in case of LCS concrete: pool configuration evolution with interface structure model 2 and lower solidification temperature tmth= 12.92 days

The impact of the second interface model leading also to an uniform heat flux profile along the concrete interface remains low; however again the choice of a lower solidification temperature and a lower upper wall temperature increases significantly the upwards radiated power thus delaying the melt-through (see fig.14 compared to fig.13).

The impact of a higher pressure is completely negligible since no stratification with metal layer below occurs with LCS concrete.

2.4 Synthesis of results

Results on the melt-through times in case of siliceous concrete are displayed in figure 15.

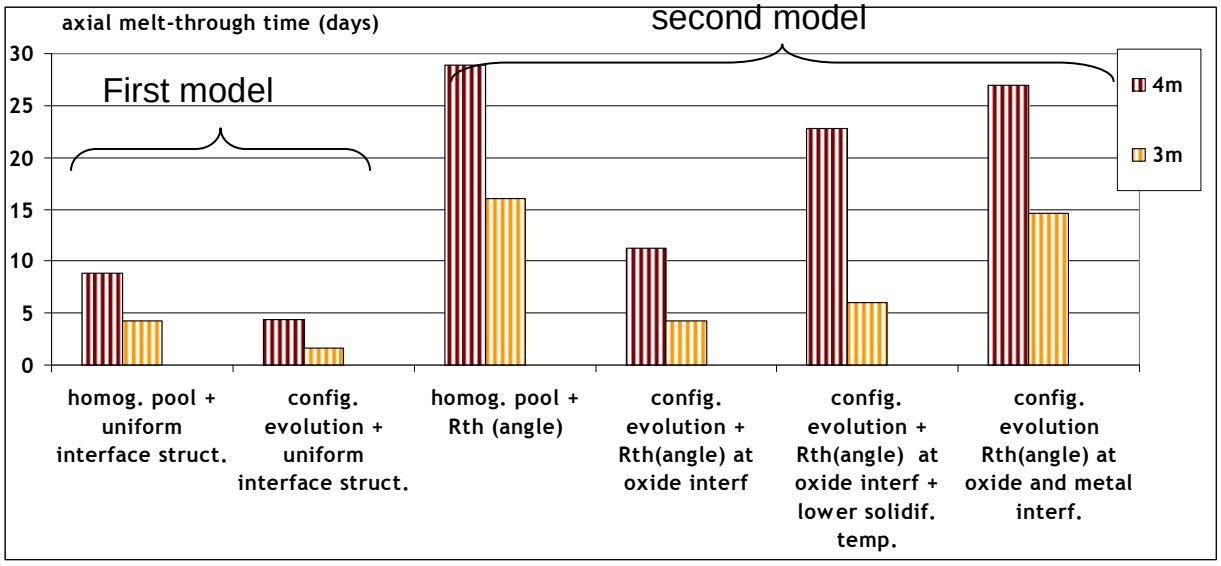

Fig.15: melt-through time for different pool/concrete interface models and pool configuration evolutions in case of siliceous concrete at low pressure

In case of a fixed homogeneous pool configuration, the axial melt-through time for a siliceous concrete basemat thickness of 4m is at minimum 9 days and is delayed beyond 20 days if taking into account a reduced thermal resistance at the bottom interface as observed in 2D MCCI experiments.

In case of pool configuration evolution with possible stratification, the axial melt-through time for a siliceous concrete 4m thick basemat is at minimum 4 days and is delayed beyond 9 days if taking into account a reduced thermal resistance at the bottom interface as observed in 2D MCCI experiments. This confirms the large impact of the new interface structure model leading to a prevailing lateral ablation in the homogeneous pool already pointed out in the previous study [1]. However the impact on the melt-through delay is still higher in this new study : indeed the more realistic stratification criterion used here increases the duration of the homogeneous pool final phase enhancing the lateral ablation at the expense of that of the stratified pool phase inducing a fast axial ablation rate. Besides in the latter case, the faster lateral ablation should cause an early lateral melt-through (before 2 days) because a minimal lateral wall thickness of 2m is eroded above the reactor pit ground. This axial melt-through which is ignored in present calculations might thus possibly decrease the corium inventory by around 20% and still delays further the axial melt-through by several days. Taking into account either the plausible build-up of a solid accumulation present both at the oxide and metal/concrete bottom interface or a slightly lower but realistic temperature of reactor pit upper structures delays the axial melt-through beyond 22 days.

Axial melt-through times obtained for the limestone-sand concrete are summarized on fig.16.

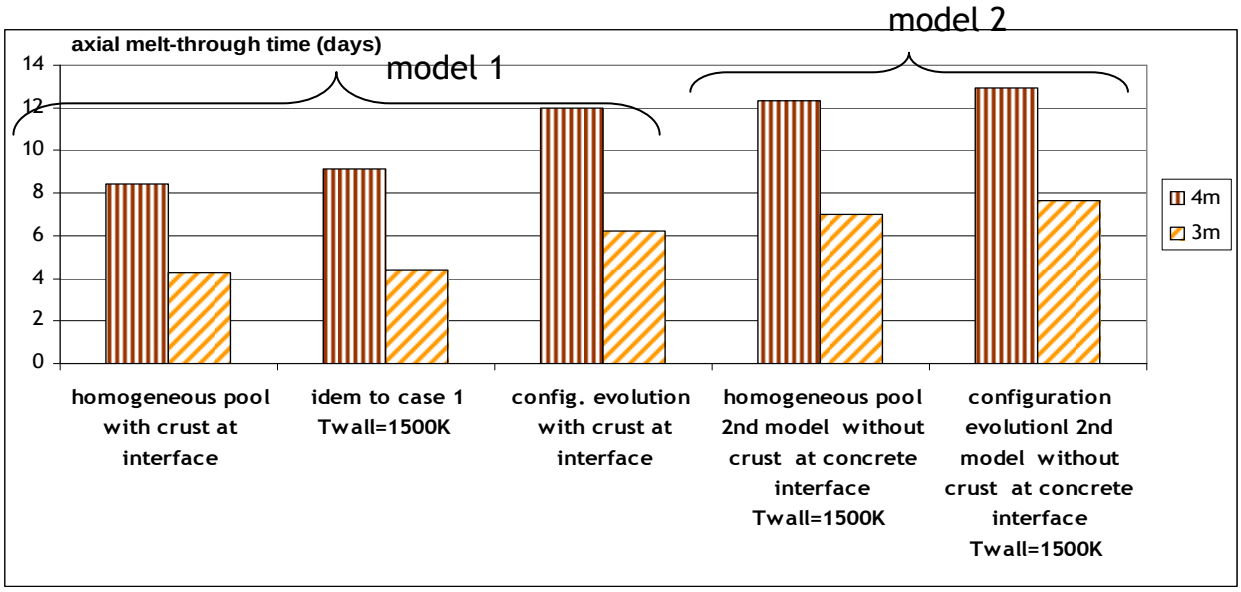

Fig.16: melt-through time for different pool/concrete interface models and pool configuration evolutions in case of LCS concrete

In case of LCS concrete, due to the likely isotropic ablation in the homogeneous pool configuration, the axial melt-through obtained with the model 2 might be earlier than with siliceous concrete (around 12 days instead of more than 20 days). Moreover a lateral ablation of at least 2m above the reactor pit ground is unlikely: the reason is the faster decrease of the corium pool upper surface due to the large reduction of concrete specific volume at ablation because of the high carbonate content. This is true in dry conditions but in case of top water injection, the corium quenching is far more efficient in case of LCS concrete due to the enhanced melt eruption process, shifting the axial melt-through for a 4m basemat thickness well beyond 20 days as shown in the previous work [1].

3 Conclusions

Reactor calculations have been performed with the ASTEC/MEDICIS code to take into account main outcomes of the 2D MCCI experimental database. It must be emphasized that values of axial melt-through times are given here only as trends for a generic 900MWe reactor and must not be considered as best-estimate values.

Main experimental data concern the 2D ablation and the pool temperature evolution during MCCI and the impact of the concrete composition on the 2D ablation. The interpretation of experiments permits to propose an improved pool/concrete interface model. At the opposite of the previous model ,this interface model is not related to the corium solidification and involves, in case of a siliceous concrete or more generally a concrete releasing intact aggregates at the ablation threshold, a non uniform thermal resistance profile along the interface with a large increase at the bottom interface and, in case of LCS concrete or concrete with aggregates losing their integrity at the ablation threshold, a uniform thermal resistance profile along the interface.

Reactor calculations performed for a typical 900Mwe reactor are using previous and new models for the pool/concrete interface structure and are focussed on the case of siliceous concrete possibly promoting the pool stratification and a fast axial ablation kinetics. Main trends derived are the following:

1) in case of siliceous concrete and for a basemat thickness of 4m, the axial melt-through time obtained with the new pool/concrete interface model reproducing the prevailing lateral ablation in the homogeneous pool configuration stays in the range from 9 to 22 days in dry conditions according to the choice of corium solidification temperature, pressure and temperature boundary conditions. The impact of the prevailing lateral ablation induced by the new model is shown to be still higher than in the previous work (1] mainly because of the more realistic stratification criterion retained here. When taking into account the possible lateral melt-through, the melt-through will still delayed by several days. Nevertheless, the impact of corium quenching is low to moderate for this concrete type [1].

2) in case of limestone-sand concrete and for a basemat thickness of 4m, pool stratification with metal below is excluded if using the above mentioned stratification criterion; the axial melt-through obtained with the new interface structure model stays around 12 days and might be earlier than with siliceous concrete due to the isotropic ablation in the homogeneous pool configuration. Moreover a lateral melt-through leading to a significant corium voiding is unlikely at the opposite of siliceous concrete. However in case of top water injection, the corium quenching is far more efficient for this concrete as

shown in [1] and shifts the axial melt-through by at least another ten days for a 4m basemat thickness, thus compensating the draw-back of isotropic ablation during the homogeneous pool phase.

The main limitation of the results presented here is the parametric nature of models used, thus questioning their validity at large scale and in the long term. However the basic underlying assumptions, in particular the absence of crust along the lateral oxidic corium/concrete interface and the build-up of the upper crust at a solidification temperature determined by a volume liquid fraction were shown to be promising when applied to the 2D MCCI experimental database. The most uncertain point is the long term behaviour of the initially built-up crust or solid accumulation at the bottom interface: this question should be answered by building more mechanistic models of the long term evolution and dissolution of this solid accumulation and if possible by performing some additional large scale 2D MCCI tests completing the MCCI2 phase program.

Once the validation of the stratification criterion proposed here is enough checked possibly by additional analytical experiments and If the prevailing lateral ablation in case of homogeneous pool is confirmed in case of a siliceous concrete and more generally for any concrete with a low gas content promoting the pool stratification, it will be possible to exclude definitely an early melt-through (less than around 5 days) due to the pool stratification occurrence provided the basemat thickness is at least 3m. Furthermore for a 4m basemat thickness, it will be permitted to conclude that the axial melt-through is shifted surely beyond 12 days and possibly beyond 20 days for any concrete type. However MCCI will not stop definitely at least in dry conditions: this points out the need of investigating MCCI mitigation issue using existing or new devices involving top and/or bottom water injection.

4 References

1) M. Cranga, B. Michel, F. Duval, C. Mun, Relative impact of MCCI modeling uncertainties on reactor basemat ablation kinetics, MCCI-OECD seminar, Cadarache, St-Paul lez Durance, France, October 10-11th 2007

2) M. Cranga, R. Fabianelli, F. Jacq, M. Barrachin, F. Duval, The MEDICIS code, a versatile tool for MCCI modelling, Proceedings of ICAPP05, Seoul, Korea, May 15-19th 2005

3) M. T. Farmer, S. Lomperski, The results of the CCI2 reactor material experiment investigating 2-D core-concrete interaction and debris coolability , 11th International Topical Meeting on Nuclear Reactor Thermal-hydraulics (NURETH-11), Avignon, France, October 2-6 2005

4) M. T. Farmer, S. Lomperski, S. Basu, A summary of findings from the melt coolability and concrete interaction (MCCI) program , Proceedings of ICAPP07, Nice, France, May 13-18th 2007

5) C. Journeau et al, "Behaviour of nuclear reactor pit concretes under severe accident conditions", Proc. CONSEC '07, Concrete under Severe Conditions, Tours, France (2007)

6) C. Journeau, P. Piluso, , J.F. Haquet, E. Boccaccio, V. Saldo, J.-M. Bonnet, S. Malaval, L. Carénini, L. Brissonneau, Two-dimensional interaction of oxidic corium with concretes: The VULCANO VB Test Series, Annals of Nuclear Energy, 36, pp.1597-1613, 2009

7) M. Cranga, C. Mun, B. Michel, F. Duval, M. Barrachin, Interpretation of real material 2D MCCI experiments in homogeneous oxidic pool with the ASTEC/MEDICIS code, Proceedings of ICAPP08, Anaheim, California, June 8-12th 2008

8) C. Journeau et al, Separate Effect Tests with Artificial Concretes to Determine the Causes of Ablation Anisotropy, MCCI-OECD seminar, Cadarache, St-Paul lez Durance, France, November 15-17th 2010

9) M. Cranga, C. Mun, C. Marchetto, MCCI in an oxidic pool: lessons learnt from MCCI-OECD and VULCANO real material experiments in dry conditions, MCCI-OECD seminar, Cadarache, St-Paul lez Durance, France, November 15-17th 2010

10) C. Journeau, J-M Bonnet, L. Ferry, J.F. Haquet, P. Piluso, Interaction of concretes with oxide+metal corium : the VULCANO VBS Series, ICAPP09, Tokyo, Japan, 2009

11) C. Journeau et al, The VULCANO Oxide-Metal Corium Concrete Interaction Experiments, MCCI-OECD seminar, Cadarache, St-Paul lez Durance, France, November 15-17th 2010

12) M. Cranga, L Ferry, J.F. Haquet, C. Journeau, B. Michel, C. Mun, P. Piluso, G. Ratel, K. Atkhen, "MCCI in an oxide-metal pool: lessons learnt from VULCANO, Greene and BALISE experiments ", ERMSAR-10 Conference, Bologne Italy, May 11-12th 2010

13) G.A. Greene and T.F. Irvine, Heat transfer between stratified immiscible liquid layers driven by gas bubbling across the interface, ANS Proceedings of the National Heat Transfer Conference, Houston, TX, July 24-27 1988

14) B. Tourniaire, J.M. Seiler, J.M. Bonnet, Study of the mixing of immiscible liquids, results of the BALISE experiments, 10th International Topical Meeting on Nuclear Reactor Thermal Hydraulics (NURETH-10), Seoul, Korea, October 5-9, 2003

15) J.M. Bonnet, Thermal hydraulic phenomena in corium pools for ex-vessel situations: the BALI experiment, Proceedings of ICONE8, 8th Int. Conf. on Nuclear Engineering, April 2-6, 2000, Baltimore, USA

16) M. Epstein, D .J. Petrie, J.H. Linehan, G .A. Lambert, D.H. Cho, Incipient stratification and mixing in aerated liquid-liquid or liquid-solid mixtures, Chemical Engineering Science, 36, pp.784-787 (1981)

17) B. Cheynet, P. Chaud, PY. Chevalier, E. Fischer, P. Mason, M. Mignanelli, NUCLEA "propriétés - dynamiques et équilibres de phases dans les systèmes d'intérêt nucléaire". In: Journal de Physique IV - France, 113, 61-64, 2004